

Photon Pair Generation with Tailored Frequency Correlations in Graded-Index Multimode Optical Fibers

HAMED POURBEYRAM^{1,2} AND ARASH MAFI^{1,2,*}

¹Department of Physics & Astronomy, Univ. of New Mexico, Albuquerque, NM 87131, USA

²Center for High Technology Materials, Univ. of New Mexico, Albuquerque, NM 87106, USA

*Corresponding author: mafi@unm.edu

Compiled April 5, 2024

We study theoretically the generation of photon pairs with controlled spectral correlations via the four-wave mixing (FWM) process in graded-index multimode optical fibers (GIMFs). We show that the quantum correlations of the generated photons in GIMFs can be preserved over a wide spectral range for a tunable pump source. Therefore, GIMFs can be utilized as quantum-state-preserving tunable sources of photons. In particular, we have shown that it is possible to generate factorable two-photon states, which allow for heralding of single-photon pure-state photons without the need for spectral post filtering. We also elaborate on the possibility of simultaneously generating correlated and uncorrelated photon pairs in the same optical fiber. © 2024 Optical Society of America

OCIS codes: (270.0270) Quantum optics; (270.5585) Quantum information and processing; (190.4380) Nonlinear optics, four-wave mixing; (060.4370) Nonlinear optics, fibers

The ability to control the coherent dynamics of photons and correlations among them paves the way to generate a wide range of quantum states from heralded single photons to entangled photon pairs. FWM in optical fibers has been used to spontaneously generate correlated photon pairs [1–9]. These signal-idler photons, sometimes referred to as *daughter* photons, share some information due to the conservation of energy and momentum. The photon pair correlations can be manipulated via tailoring the joint spectral amplitude (JSA) of the photon pair [5, 10–14], giving access to a variety of quantum states, from a highly correlated photon pair (entangled) [15] to an uncorrelated pair (factorable) that can be used as a heralded pure-state single photon source [16, 17].

The extra degrees of freedom available in multimode optical fibers can be used to control the physical attributes of the photon pairs generated via the spontaneous FWM process. The presence of multiple spatial modes allows for the intermodal FWM (IM-FWM) process, which can result in signal and idler photons that have large spectral separations from the pump [18–20]; therefore, they are minimally contaminated by the scattered and residual pump and Raman photons. Different spatial mode combinations can also result in different IM-FWM processes that allow for the

simultaneous generation of multiple photon pairs in the same fiber [7, 14]. The diversity of the group velocities of different spatial modes can also be used as an effective tool to manipulate the JSA of the photons pairs.

Among the general class of MMFs, GIMFs exhibit unique dispersive, nonlinear, and spatiotemporal properties [21–24]. For example, their modes can be classified into mode-groups with identical intra-group and equally-spaced inter-group phase velocities [21, 25]. All modes can also be designed to have nearly identical group velocities near a special wavelength [21]. Therefore, short high peak power laser pulses do not easily disintegrate due to intermodal group velocity dispersion and the laser pulses go through a rapid submillimeter-length self-imaging pattern when propagating along these fibers [26]. These unique properties make GIMFs an appealing platform for observing novel nonlinear optic phenomena. Examples include the observation of multimode solitons [27, 28], supercontinuum generation [29, 30], multimode saturable absorption [31], self-induced beam cleanup [29, 32], and geometric parametric instability [33–35]. In this paper, we leverage the unique dispersive and nonlinear properties of GIMFs for the generation of photon-pair states with a high degree of control over their spectral correlations for an ultra-broad spectral range.

We recently explored the tailoring of the JSA of the photon pair generated in a commercial multimode step-index optical fiber via the IM-FWM process [14]. We showed that it is possible to generate factorable two-photon states exhibiting minimal spectral correlations between the photon pair components in conventional multimode fibers using commonly available pump lasers. In this paper, we extend our studies to the case of photon pair generation in GIMFs. We show that a commercial GIMF can be used as a robust medium to generate factorable photon pairs over a large bandwidth that can be considerably larger than that obtained in step-index fibers. This interesting property is rooted in the special dispersive attributes of GIMFs.

We first present a brief overview of GIMFs and establish the notation that will be used in the rest of the paper. The refractive index profile of a GIMF is given by

$$n^2(\rho) = n_0^2 \left[1 - 2\Delta \left(\frac{\rho}{R} \right)^\alpha \right]. \quad (1)$$

R is the core radius, n_0 is the refractive index in the center of the core, Δ is the relative index difference between the core and

cladding, $\alpha \approx 2$ characterizes a near parabolic-index profile in the core ($\rho \leq R$), and $\alpha = 0$ in the cladding ($\rho > R$).

The guided linearly polarized (LP) modes are represented by Laguerre-Gaussian functions [21]. Each mode is identified by two integers, p , and m , referred to as the radial and angular numbers, respectively. In this notation, each mode is shown in the form $LP_{|m|,p+1}$. The mode-group number is also defined as $g = 2p + |m| + 1$. All the guided modes with an identical mode-group number g are nearly degenerate in the value of their propagation constant β_g [21, 25] defined by

$$\beta_g = n_0 k (1 - 2N\Delta)^{1/2}, \quad (2)$$

$$N = \left(\frac{g}{\sqrt{N_\alpha}} \right)^{2\alpha/(\alpha+2)}, \quad N_\alpha = \frac{\alpha}{\alpha+2} n_0^2 k^2 R^2 \Delta. \quad (3)$$

N_α indicates the total number of guided modes (considering the polarization degeneracy), and $k = 2\pi/\lambda$, where λ is the wavelength. For the calculations in this paper, we have considered a commercial GIMF with typical parameters which can be found in Refs. [21, 25]. Briefly, $R = 25 \mu\text{m}$, $\Delta = 0.01$, and $\alpha \approx 2.11$.

The phase-matching for IM-FWM is given by

$$\beta_v^p + \beta_\kappa^p - \beta_\mu^s - \beta_\xi^i = 0, \quad (4)$$

where the superscripts signify the pump (p), signal (s), and idler (i). The subscripts index the specific Laguerre-Gaussian spatial mode in which the pump, signal, or idler propagate. Because the propagation constants only depend on the mode-group numbers (see Eq. (2)), the phase matching can be readily cast into a relationship among the mode-group numbers $\{g_p^{(1)}, g_p^{(2)}, g_i, g_s\}$, representing the two pump photons, the idler photon, and the signal photon, respectively.

The JSA of the signal-idler photon pair generated in a optical fiber can be constructed [11, 14, 36] using the group delay between pump-signal and pump-idler photons given by

$$\tau_j = L [\beta_p^{(1)}(\bar{\omega}_p) - \beta_j^{(1)}(\bar{\omega}_j)], \quad j \in \{s, i\}, \quad (5)$$

and the pump bandwidth σ_p . L is the fiber length. In Eq. (5) $\beta_j^{(1)}$ is the inverse of the group velocity defined as $\partial\beta/\partial\omega$, and $\bar{\omega}_j$ ($j \in \{p, s, i\}$) indicate the phase-matched frequencies. Using τ_s , τ_i , and σ_p , it is possible to determine the correlation among signal and idler by calculating the purity of the quantum state, \mathcal{P} , for idler (or signal) photon. The explicit form of \mathcal{P} is given by [14]

$$\mathcal{P} = \sqrt{\frac{2\eta r_2^2 (X_1 - 2)X_1}{(2r_2^2 X_1 + \eta r_1)(2r_2^2 X_1 + \eta/r_1)}}, \quad \eta \approx 0.193, \quad (6)$$

which is parameterized using two dimensionless parameters r_1 and r_2 defined as

$$r_1 = \frac{\tau_s}{\tau_i}, \quad r_2 = \frac{\sigma_{si}}{\sigma_p}, \quad \sigma_{si} = \frac{1}{\sqrt{\tau_s^2 + \tau_i^2}}, \quad X_1 = r_1 + \frac{1}{r_1}. \quad (7)$$

Note that \mathcal{P} ranges from unity to zero, where a pure quantum state ($\mathcal{P} = 1$) indicates a spectrally uncorrelated signal-idler photon pair, giving a factorable quantum state.

In Fig. 1 we show the phase-matched signal-idler frequencies (ν_s and ν_i) as a function of pump frequency (ν_p), for two FWM processes in the GIMF. In this figure, $\{g_p^{(1)}, g_p^{(2)}, g_i, g_s\} = \{1, 1, 1, 3\}$ is labeled for example as $\{1, 1, 1, 3\}$. There is clearly

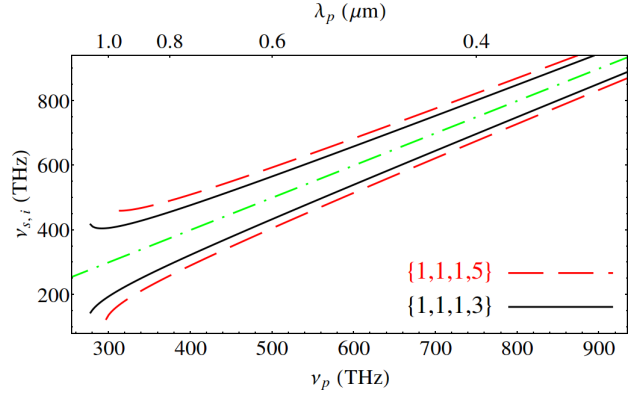


Fig. 1. Phase-matched FWM frequencies ν_s, ν_i as a function of pump frequency ν_p ($\nu_j = \omega_j/2\pi$), for two distinct FWM processes. The dot-dashed green line represents the pump line.

a linear dependence of $\bar{\omega}_s$ ($\bar{\omega}_i$) versus $\bar{\omega}_p$ over a wide range of pump spectrum for all depicted processes. It can be generally shown that [14, 37]

$$r_1 = 1 - 2 \frac{d\bar{\omega}_p}{d\bar{\omega}_s}; \quad (8)$$

therefore, according to Eq. (8), if $d\bar{\omega}_p/d\bar{\omega}_s$ does not change with varying the pump wavelength (as is the case for a broad spectral range in Fig. 1), the value of r_1 does not change with the pump wavelength. Therefore, the value of purity can be easily kept constant by keeping r_2 unchanged by merely rescaling the length of the fiber L . Later, we will show that $r_1 \approx -1$ is easily accessible for GIMFs; therefore, one can generate an ultra-broadband tunable photon pair source with $\mathcal{P} \approx 1$ by the judicious selection of L or σ_p .

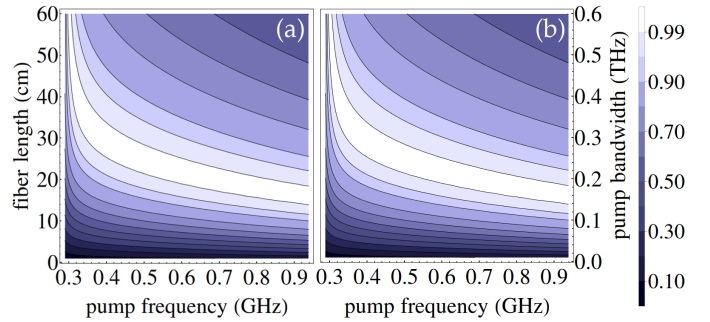


Fig. 2. Purity contours as a function of pump frequency ν_p vs. (a) fiber length for fixed pump bandwidth of 0.5 THz, and (b) pump bandwidth for a 50 cm long fiber. Both contours are for $\{1, 1, 1, 3\}$ process.

In Fig. 2, we demonstrate our theoretical calculation of purity as a function of the pump frequency versus the (a) fiber length, and (b) pump bandwidth. The calculations are performed for the $\{1, 1, 1, 3\}$ process. In Fig. 2(a), it can be seen that for the fixed value of σ_p , $\mathcal{P} \approx 1$ can be achieved by tuning the value of L . Moreover, even if the value of L is kept fixed, it is possible to maintain high purity over a reasonably large pump frequency range, making it highly desirable from a device standpoint. A similar argument can be made in Fig. 2(b) by reversing the role of L and σ_p .

The results presented in Fig. 2 are for the $\{1, 1, 1, 3\}$ process. In

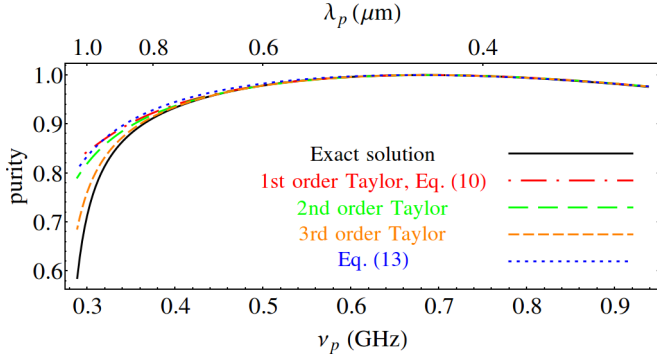


Fig. 3. Purity vs. pump frequency using different methods discussed. The spectral separation is for {1,1,1,3} process, $G=2$, fiber length is 50 cm, and pump bandwidth is 0.2 THz.

the following, we will show that the value of purity in GIMFs, in general, depends mainly on the spectral separation of the signal/idler from the pump (Ω). This is an important result from an experimental standpoint because one will not even need to examine the mode profiles and can evaluate the value of the purity expected from the process only by a simple spectral measurement. From a theoretical standpoint, this result is interesting because the frequency separation is analytically calculable knowing the mode-group numbers involved in the FWM process [25].

In order to show that the purity in GIMFs depends mainly on Ω , we expand Eq. (2) to the first order in the small parameter Δ and obtain

$$\beta_g \approx n_0(\lambda)k - \frac{\sqrt{2\Delta}}{R}g. \quad (9)$$

Because terms of higher orders in Δ have been ignored, this approximation is only reliable if the length of the fiber L satisfies $L \ll L_0/g^2$, where $L_0 = \pi n_0 k R^2 / \Delta$ [21]. For the commercial GIMF in Refs. [21, 25], we have $L_0 \approx 2.2$ m at $\lambda = 850$ nm. Therefore, this approximation holds for the typical fiber lengths considered in this paper for photon pair generation. Using Eq. (9) and ignoring the frequency dependence of Δ , we have $\beta^{(1)} = \partial_\omega(n\omega/c)$; therefore, the group velocity is independent of the group number g . Furthermore, we can expand the $\beta^{(1)}$ belonging to the signal (idler) around the $\bar{\omega}_p$ and only keep the terms up to the first order in the signal/idler-pump frequency separation Ω to get even a more simplified equation for the group delay τ . We will discuss the validity of these approximations later in this paper. In this case, the group delays can be written as

$$\tau_s \approx +\Omega \frac{L}{c} \partial_\omega^2(n\omega)|_{\bar{\omega}_p}, \quad \tau_i \approx -\Omega \frac{L}{c} \partial_\omega^2(n\omega)|_{\bar{\omega}_p}. \quad (10)$$

In GIMFs, Ω can be accurately estimated using the material dispersion and physical parameters of the fiber by [25]

$$\Omega^2 \approx \frac{\sqrt{2\Delta}}{R} \frac{Gc}{\partial_\omega^3(n\omega)}, \quad (11)$$

where $G = g_s + g_i - g_p^{(1)} - g_p^{(2)}$. G is determined by the modes involved in the FWM process, e.g. $G = 2$ is used for the FWM process identified by {1,1,1,3}. Using Eqs. (10) and (11), r_1 and r_2 simplify to

$$r_1 \approx -1, \quad r_2 \approx \frac{1}{\sigma_p L} \sqrt{\frac{Rc}{G\sqrt{8\Delta}}} \left[\partial_\omega^2(n\omega) \right]^{-\frac{1}{2}}, \quad (12)$$

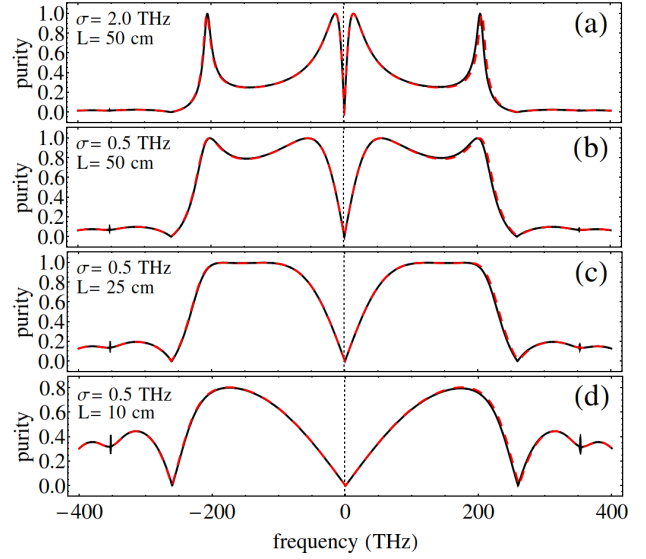


Fig. 4. Purity as a function of spectral separation from the pump. Dashed red line indicates the result calculated using Eq. 10, and the solid black line shows the result calculated from an exact form of the propagation constant in Eq. (2) for {1,1,1,3}.

from which the purity is calculated as

$$\mathcal{P} = \frac{4r_2\sqrt{\eta}}{4r_2^2 + \eta}. \quad (13)$$

We emphasize that in order to use these approximations, it is important for the modes involved in the FWM process to be far from their cutoff frequencies such that the material dispersion dominates over the waveguide contribution.

In Fig. 3, we examine the accuracy of the approximations made so far in detail. We consider the purity calculation for the {1,1,1,3} process ($G = 2$) for the fiber length of 50 cm and the pump bandwidth of 0.2 THz as a function of the pump frequency ν_p . The solid (black) curve shows the full calculation using Eq. (2) and its derivatives, so no approximation is made. The dashed-dotted (red) curve uses the approximation in Eqs. (10), for which the value of Ω is calculated directly by using Eq. (2). The long-dashed (green) and short-dashed (cyan) curves are calculated in a similar way to the dashed-dotted (red) curve except 2nd and 3rd order Taylor expansion terms in Eq. (10) are retained. The dotted (purple) curve is plotted using the full approximation formula in Eq. (13) where Ω is calculated using the approximation in Eq. (11). Therefore, there is a good agreement between the exact solution and these approximate methods for a wide range of the pump frequency. Results presented in Fig. 3 also show more clearly the possibility of a tunable uncorrelated photon pair source in a GIMF.

According to the approximations presented earlier, we argued that the purity is determined chiefly by the spectral separation Ω , and the dependence on the mode-groups numbers appears only indirectly through Ω and Eq. (11). Therefore, from a practical standpoint in an experiment, where one usually measures the FWM spectrum rather than the modal content, it is interesting to investigate the purity only as a function of Ω for various experimental scenarios. This is done in Fig. 4 where purity is plotted as a function of Ω for several different values of L and σ_p for the photon pairs generated through the {1,1,1,3} pro-

cess using an 850 nm wavelength pump. In each subfigure, the dashed red line demonstrates the approximate calculation from Eq. (10), and the solid black line shows the calculation using the exact form of the group velocity. It must be noted that these should be treated as general reference plots; the exact modal content will fix the value of Ω at a particular phase-matched frequency shift. The fact that the approximate method (applicable to all values of G) and the exact method (only applicable to {1,1,1,3} though ignoring the phase-matching) give nearly identical results prove the broad applicability of these curves. Moreover, different scenarios show that by a proper choice of L and σ_p it is possible to have high purity over a broad spectral band; or obtain high purity in one frequency region and low purity in another. Therefore, it is possible to simultaneously generate mixed purity values using different multimode phase-matching processes in a single strand of optical fiber.

In conclusion, we have investigated GIMFs as an ultra-broadband source of photon pairs with controlled spectral correlations. We show that GIMFs can be used as a tunable source of uncorrelated (or correlated) photon pairs as their spectral correlations are relatively independent of the pump central wavelength. Our calculations indicate that while tuning the pump frequency will change the frequencies of the signal and idler, the signal (idler) photon state purity remains unchanged. Therefore, GIMFs can be used to make quantum-state-preserving tunable sources of photon pairs. We have also shown that the purity is mainly a function of the spectral separation of the idler-signal pair from the pump (Ω), and its dependence on the spatial mode content is indirect and only through its dependence on Ω . Finally, we have shown that by the right selection of the physical parameters of the system including the fiber length and/or the pump bandwidth, it is possible to simultaneously generate correlated and uncorrelated photon pairs in the same optical fiber.

ACKNOWLEDGMENT

The authors acknowledge support by the National Science Foundation (NSF) Grant No. 1522933.

REFERENCES

1. X. Li, P. L. Voss, J. E. Sharping, and P. Kumar, *Phys. Rev. Lett.* **94**, 053601 (2005).
2. J. G. Rarity, J. Fulconis, J. Duligall, W. J. Wadsworth, and P. S. J. Russell, *Opt. Express* **13**, 534 (2005).
3. Q. Lin, F. Yaman, and G. P. Agrawal, *Opt. Lett.* **31**, 1286 (2006).
4. E. A. Goldschmidt, M. D. Eisaman, J. Fan, S. V. Polyakov, and A. Migdall, *Phys. Rev. A* **78**, 013844 (2008).
5. O. Cohen, J. S. Lundeen, B. J. Smith, G. Puentes, P. J. Mosley, and I. A. Walmsley, *Phys. Rev. Lett.* **102**, 123603 (2009).
6. B. Fang, O. Cohen, and V. O. Lorenz, *J. Opt. Soc. Am. B* **31**, 277 (2014).
7. D. Cruz-Delella, J. Monroy-Ruz, A. M. Barragan, E. Ortiz-Ricardo, H. Cruz-Ramirez, R. Ramirez-Alarcon, K. Garay-Palmett, and A. B. U'Ren, *Opt. Lett.* **39**, 3583 (2014).
8. R. A. Smith, D. V. Reddy, D. L. Vitullo, and M. G. Raymer, *Opt. Express* **24**, 5809 (2016).
9. R. J. A. Francis-Jones, R. A. Hoggarth, and P. J. Mosley, *Optica* **3**, 1270 (2016).
10. W. P. Grice, A. B. U'Ren, and I. A. Walmsley, *Phys. Rev. A* **64**, 063815 (2001).
11. K. Garay-Palmett, H. J. McGuinness, O. Cohen, J. S. Lundeen, R. Rangel-Rojo, A. B. U'ren, M. G. Raymer, C. J. McKinstrie, S. Radic, and I. A. Walmsley, *Opt. Express* **15**, 14870 (2007).
12. J. B. Christensen, C. McKinstrie, and K. Rottwitt, *Physical Review A* **94**, 013819 (2016).
13. L. Cui, X. Li, and N. Zhao, *New Journal of Physics* **14**, 123001 (2012).
14. H. Pourbeyram and A. Mafi, *Phys. Rev. A* **94**, 023815 (2016).
15. X. Li, J. Chen, P. Voss, J. Sharping, and P. Kumar, *Opt. Express* **12**, 3737 (2004).
16. C. Söller, O. Cohen, B. J. Smith, I. A. Walmsley, and C. Silberhorn, *Phys. Rev. A* **83**, 031806 (2011).
17. B. Fang, O. Cohen, J. B. Moreno, and V. O. Lorenz, *Opt. Express* **21**, 2707 (2013).
18. C. Lin and M. A. Bösch, *Applied Physics Letters* **38**, 479 (1981).
19. H. Pourbeyram, E. Nazemosadat, and A. Mafi, *Opt. Express* **23**, 14487 (2015).
20. R. Dupiol, A. Bendahmane, K. Krupa, A. Tonello, M. Fabert, B. Kibler, T. Sylvestre, A. Barthélemy, V. Couderc, S. Wabnitz, and G. Millot, *Opt. Lett.* **42**, 1293 (2017).
21. A. Mafi, *J. Lightwave Technol.* **30**, 2803 (2012).
22. L. G. Wright, D. N. Christodoulides, and F. W. Wise, *Nature Photonics* **9**, 306 (2015).
23. S. Buch and G. P. Agrawal, *J. Opt. Soc. Am. B* **33**, 2217 (2016).
24. L. G. Wright, D. N. Christodoulides, and F. W. Wise, *Science* **358**, 94 (2017).
25. E. Nazemosadat, H. Pourbeyram, and A. Mafi, *J. Opt. Soc. Am. B* pp. 144–150.
26. A. Mafi, P. Hofmann, C. J. Salvin, and A. Schülzgen, *Opt. Lett.* **36**, 3596 (2011).
27. L. G. Wright, W. H. Renninger, D. N. Christodoulides, and F. W. Wise, *Opt. Express* **23**, 3492 (2015).
28. Z. Zhu, L. G. Wright, D. N. Christodoulides, and F. W. Wise, *Opt. Lett.* **41**, 4819 (2016).
29. G. Lopez-Galmiche, Z. S. Eznavah, M. A. Eftekhari, J. A. Lopez, L. G. Wright, F. Wise, D. Christodoulides, and R. A. Correa, *Opt. Lett.* **41**, 2553 (2016).
30. K. Krupa, C. Louot, V. Couderc, M. Fabert, R. Guenard, B. M. Shalaby, A. Tonello, D. Pagnoux, P. Leproux, A. Bendahmane, R. Dupiol, G. Millot, and S. Wabnitz, *Opt. Lett.* **41**, 5785 (2016).
31. E. Nazemosadat and A. Mafi, *J. Opt. Soc. Am. B* **30**, 1357 (2013).
32. H. Pourbeyram, G. P. Agrawal, and A. Mafi, *Applied Physics Letters* **102**, 201107 (2013).
33. S. Longhi, *Opt. Lett.* **28**, 2363 (2003).
34. K. Krupa, A. Tonello, A. Barthélemy, V. Couderc, B. M. Shalaby, A. Bendahmane, G. Millot, and S. Wabnitz, *Phys. Rev. Lett.* **116**, 183901 (2016).
35. U. Teğin and B. Ortaç, *arXiv preprint arXiv:1705.09157* (2017).
36. B. J. Smith, P. Mahou, O. Cohen, J. S. Lundeen, and I. A. Walmsley, *Opt. Express* **17**, 23589 (2009).
37. O. Cohen, "Generation of uncorrelated photon-pairs in optical fibres," Ph.D. thesis, University of Oxford (2010).